4

IR Support of Thermophysical Property Investigation – Study of Medical and Advanced Technology Materials

Andrzej J. Panas
Military University of Technology,
Air Force Institute of Technology
Poland

1. Introduction

In spite of a huge advance in thermophysical property [TP] investigation technology and instrumentation there are still areas where we experience lack of precise information concerning heat transfer characteristics of certain materials or structures. Many biological or medical technology materials (see eg. Lin at al., 2010a or O'Brien, 1997) can be indicated as good examples. The same concerns some of the advanced technology materials and structures. The reasons for that are difficulties in obtaining the adequate specimens as well as complicated composition and structure of the studied materials which make the standard measurements more difficult. Since standard technologies of thermophysical property investigation are based on analytical models of regular geometry, they need regular specimens of a certain dimension (comp. Maglić et all, 1984, 1992). This is not always possible regarding the discussed materials.

For that reason, other technologies for TP investigation of non-typical materials are still being developed. Many of them take advantage of contactless temperature measurements inherent in infrared (IR) technology. Non-intrusive examination can be especially beneficial in the case of investigations of materials available only in form of thin sheets and foils, specimens of anisotropic materials, composite samples, etc. For specimens of irregular shape the most important is the possibility of inspecting a specific area with a certain spatial resolution. To perform such an inspection an IR camera is usually applied.

The infrared technique is so effective that it creates opportunity for unconventional (see eg. Perkowski, 2011) arrangement of TP investigation. However, in most cases IR cameras are applied for TP investigation just to replace traditional contact sensors (see eg. Bison at all., 2002; Miettinien at all., 2008). Using conventional methods can be justified because they are reliable and because their increased performance is usually expected when using thermal imaging. By studying high resolution data of steady-state temperature distribution instead of discrete temperature recordings one can widen the range of the on-going analysis. In the case of transient temperature measurements the spatial temperature distribution provides additional opportunity for data completion or correction. In all the cases it seems that experiments are facilitated but that is not always true.

Quantitative analysis of TP of the investigated structure should account for some negative effects inherent in IR technology like open area heat losses and systematic errors of temperature measurements because of local differences in surface properties. Violation of heat transfer phenomena symmetry should also be kept in mind concerning anisotropic, composite or irregular in shape specimens. Some of the systematic errors could be corrected by introducing additional data processing techniques ie. numerical modelling. But the most important is compensation of some IR technique disadvantages by a proper selection of the experimental TP measurement method. It seems that transient methods prevail in that domain over stationary ones because of an extended range of possibilities based on both spatial and temporal temperature distribution. Regarding transient techniques regular heating regime procedures assure less problematic temperature field excitation (comp. eg. Maglić, 1984). There are three modes of regular thermal operation (Volkhov & Kasperovich, 1984): step heating, linear heating or temperature oscillation. Usually these methods are applied for the thermal diffusivity [TD] investigation which is the key parameter in the transient thermal conductivity. It has been shown that the combination of the linear heating approach with the temperature oscillation technique (Panas & Nowakowski, 2009) provides an interesting possibility for additional study of TD dependence on the temperature. Both of them exhibit better metrological conditioning than other techniques. And last but not least, they can be easily implemented utilising relatively simple instrumentation. It should be noticed that this does not concern problems of measurements performed on micro or nano-sized particles (comp. eg. Wang & Tung, 2011). In such an instance microscope apparatus makes measurements high-priced. But it is not the reason for which we will focus our attention on macro-sized specimens only. Microscope technology measurements evoke the problem of validity of classical heat transfer theory application in such circumstances. It concerns both the issue of application of Fourier vs. non-Fourier law and, in wider perspective, even the problem of local thermal equilibrium definition.

2. Theory

Regular heating regime refers to a situation when the initial condition has negligible effect on the actual thermal state of the body (Kondratiev, 1954, as cited in Lykov, 1967). The theory of such a regime is the generalisation of well-known quasi-stationary conditions. Usually the first, second, and third kind of regimes are distinguished (Volokhov & Kasperovich, 1984; Platunov, 1992). The first two are also referred to as monotonic heating regimes. At monotonic heating the investigated specimen is heated at the constant ambient temperature (1st) or heating proceeds at the constant rate (2nd). The third kind of regular regime includes periodic heating also referred to as temperature wave technique (Phylippov, 1984). The temperature oscillation was introduced for the thermophysical property investigation of good conductors by Ångström (Ångström, 1861) but its application has also been extended to insulators (Belling & Unsworth, 1987).

There are available many mathematical models of regular heating regime problems that have been formulated in all three basic coordinate systems and solved for different dimensions (see eg. Carslaw & Jaeger, 2003; Maglić et al., 1992, 1984; Lykov, 1967). In the present study two models of the temperature oscillation are discussed: classical Ångström's solution of the longitudinal temperature oscillation in semi-infinite rod with side surface convection heat losses and modified Ångström's model (Belling & Unsworth, 1987) with

additional, linear in time temperature change imposed onto basic boundary temperature oscillation (Panas & Nowakowski, 2009). In addition a generalised model of the 1st kind monotonic heating is recalled.

For the purpose of this study we restrict to one-dimensional Cartesian coordinate system O–x formulation in all cases. To benefit from linear character of mathematical problems we also assume that the basic thermophysical properties and characteristics are constant. In practice it means that although the density ρ, specific heat c_p, and the thermal conductivity λ can be temperature dependent the changes are negligible regarding the expected maximum temperature difference within the analyzed object. The same assumption concerns the heat transfer coefficients (surface conductances): h – describing the convection heat losses taken present in the governing equation and H – present in boundary condition [BC]. Thus, the generalized governing equation for all the analyzed problems is as follows

$$\frac{\partial \theta}{\partial \tau} = a \frac{\partial^2 \theta}{\partial x^2} - \nu\theta \; ; \quad \theta(x,\tau) = T(x,\tau) - T_0 \; ; \; a = \frac{\lambda}{\rho \, c_p} \; , \quad \nu = \frac{hp}{\rho c_p S} \; , \tag{1}$$

where

$$\theta(x,\tau) = T(x,\tau) - T_0 \tag{2}$$

denotes the temperature referring to a certain T_0 value, τ is the time, a is the thermal diffusivity and ν is a constant describing the intensity of internal convection heat loses.

2.1 One-dimensional temperature oscillation in semi-infinite rod

The solution of Eq. (1) is sought within the interval $[x, \infty)$ for the rod treated as a thermally thin body of the perimeter p and cross-section area S that defines ν constant as

$$\nu = \frac{hp}{\rho c_p S} \; . \tag{3}$$

Regarding possibility of Fourier series representation of any periodic temperature variation of the angular frequency ω, the analysis in this instance can be restricted to such BCs:

$$\theta(0,\tau) = A \sin(\omega\tau + \varepsilon) \; , \qquad \lim_{x\to\infty} \theta(x,\tau) = 0 \; . \tag{4}$$

The solution, describing a developed thermodynamic process, is (Carslaw & Jaeger, 2003):

$$\theta(x,\tau) = A \, e^{-qx} \sin(\omega\tau - q'x + \varepsilon) = A \, e^{-qx} \sin(2\pi f\tau - q'x + \varepsilon) \, , \tag{5}$$

where f is the frequency, and

$$q = \sqrt{\frac{\sqrt{\nu^2 + \omega^2} + \nu}{2a}} \; , \quad q' = \sqrt{\frac{\sqrt{\nu^2 + \omega^2} - \nu}{2a}} \; . \tag{6}$$

There are several possibilities to arrange an experiment utilising the above solution for the thermal diffusivity identification (Bison at al., 2002; Phylippov, 1984). One of the

arrangement benefits from examination of the temperature oscillation attenuation ψ and the phase shift φ when passing from x_1 to x_2, $x_2 > x_1 \geq 0$ (Fig. 1):

$$\psi = \frac{\max\limits_{\tau}\left[\theta(x_2,\tau)\right]}{\max\limits_{\tau}\left[\theta(x_1,\tau)\right]} = \frac{\exp(-qx_2)}{\exp(-qx_1)} = \exp(-ql), \quad \varphi = q'(x_2 - x_1) = q' l, \; l = x_2 - x_1. \tag{7}$$

Hence the thermal diffusivity a and the convection heat transfer constant ν are given by:

$$a = \frac{\pi f}{q\, q'}, \qquad \nu = \frac{\pi f}{q\, q'}\left(q^2 - q'^2\right). \tag{8}$$

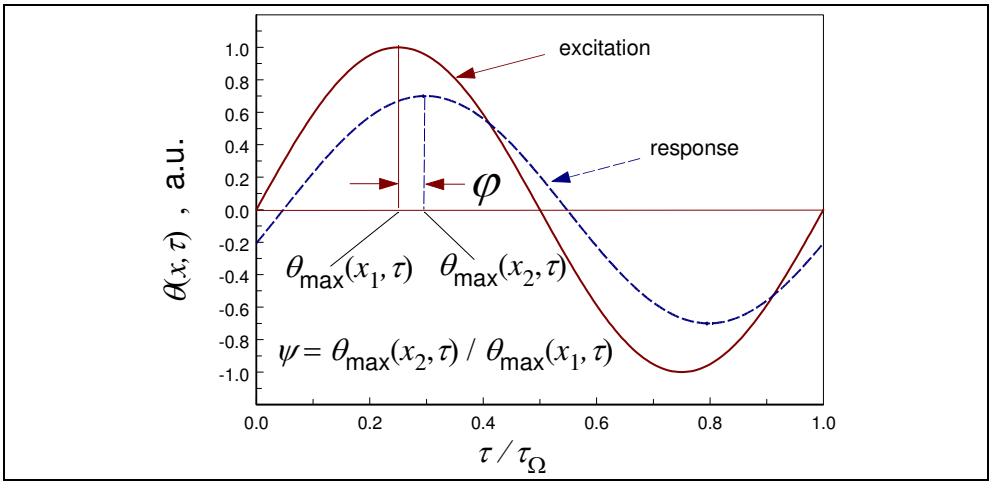

Fig. 1. Illustration of the sinusoidal temperature oscillation attenuation and lagging

Applying Eq. (7) the first relation from the two above can be rearranged into the form:

$$a = \frac{\pi f}{q\, q'} = \frac{\pi f}{\left(\frac{1}{l}\ln\frac{1}{\psi}\right)\left(\frac{\varphi}{l}\right)} = \sqrt{\frac{\pi f l^2}{\ln^2\frac{1}{\psi}}}\sqrt{\frac{\pi f l^2}{\varphi^2}} = \sqrt{a_\psi\, a_\varphi}, \tag{9}$$

where:

$$a_\psi = \frac{\pi f l^2}{\ln^2\frac{1}{\psi}} = \frac{\pi l^2}{\tau_\Omega \ln^2\frac{1}{\psi}}, \qquad a_\varphi = \frac{\pi f l^2}{\varphi^2} = \frac{\pi\, l^2}{\tau_\Omega\, \varphi^2}, \qquad \begin{cases} a_\varphi > a_\psi & \text{for } \nu > 0 \\ a_\varphi = a_\psi & \text{for } \nu = 0 \end{cases}. \tag{10}$$

Parameters a_ψ and a_φ represent the amplitude and phase apparent thermal diffusivity values. In the case when the side surface of the analysed rod is perfectly insulated, the thermal diffusivity can be obtained independently applying the amplitude attenuation and the phase shift data.

2.2 One-dimensional temperature oscillation within a slab with a linear boundary temperature drift

Developing this model we exclude internal convective heat losses (ν=0) and assume that such modified governing Eq. (1) is valid within the interval $0 \le x \le L$ where L is the slab thickness. Regarding the linearity of the discussed heat transfer problems, the generalised boundary conditions defined by the following formulae

$$\frac{\partial \theta(0,\tau)}{\partial x} = 0, \quad \theta(L,\tau) = A\sin(2\pi f\tau + \varepsilon) + b\,\tau\,, \tag{11}$$

where b is the temperature change rate, can be decomposed into two separate BC sets: the first taking into account periodic component and the second considering the right-hand boundary linear temperature change. The behaviour of the system under these conditions is illustrated in Fig. 2. The appropriate solutions for the slab with zero initial temperature can be found in monograph by Carslaw Jaeger (Carslaw & Jaeger, 2003; pp. 104-105). The final solution disregarding the initial irregular heating regime can be expressed as (Panas & Nowakowski, 2009)

$$\theta(x,\tau) = A\ \psi\ \sin(2\pi f\tau - \varphi + \varepsilon) + b\tau + \frac{b\left(x^2 - L^2\right)}{2a}. \tag{12}$$

The parameters ψ and φ have the same interpretation as in the previous case - they represent the oscillation amplitude attenuation and the oscillation phase shift respectively. However, the relations between ψ, φ and the thermal diffusivity a are now far more complicated (Carslaw & Jaeger, 2003):

$$\psi(x) = \sqrt{\frac{\cosh 2kx + \cos 2kx}{\cosh 2kL + \cos 2kL}}, \qquad \varphi(x) = \arg\left[\frac{\cosh kx(1+i)}{\cosh kL(1+i)}\right], \tag{13}$$

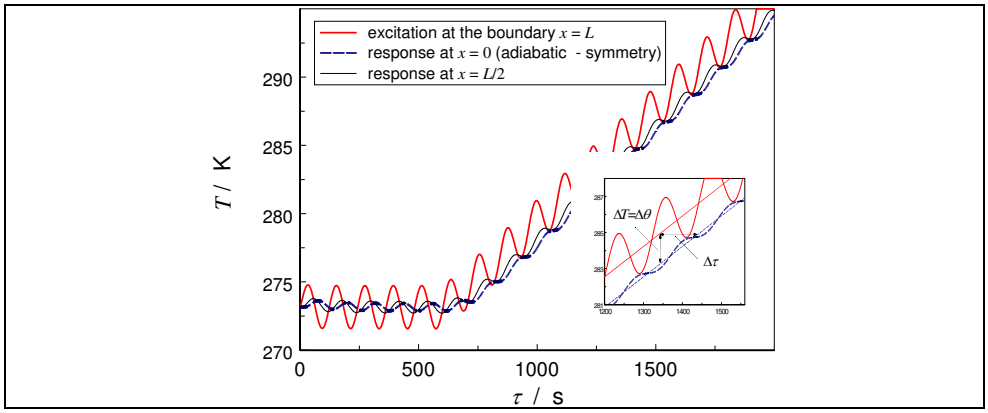

Fig. 2. Illustration of the sinusoidal temperature oscillation with a linear scan imposed from τ = 600 s (numerical modelling results of the appropriate heat transfer within the slab; Panas & Nowakowski, 2009)

where

$$k = \sqrt{\frac{\pi f}{a}} = \sqrt{\frac{\pi}{a\,\tau_\Omega}}\,. \tag{14}$$

It also should be noted that in present formulation the "thermal wave" propagates in opposite direction (the amplitude attenuates while x is decreasing from L to 0). The thermal diffusivity can be calculated on the basis of known ψ and φ by solving the transcendental Eqs. (13). The independently obtained a_ψ and a_φ when compared, can be used for cross-validation of the developed experimental procedure.

For $x = 0$, which is a typical situation during IR investigation, one can rearrange Eqs. (13) to

$$\frac{\sqrt{2}}{\psi} = \sqrt{\cosh\left(2\sqrt{\frac{\pi f}{a}}\cdot L\right) + \cos\left(2\sqrt{\frac{\pi f}{a}}\cdot L\right)}\,, \quad \tan\varphi = \tan\left(\sqrt{\frac{\pi f}{a}}\cdot L\right)\tanh\left(\sqrt{\frac{\pi f}{a}}\cdot L\right). \tag{15}$$

It was shown that these formulae can be reduced to much simpler explicit approximations:

$$a \cong \frac{\pi f L^2}{\ln^2 \frac{2}{\psi}}\,, \qquad a \cong \frac{\pi f L^2}{\varphi^2}\,, \tag{16}$$

if the oscillation frequency is high enough to fulfil the following condition (Bodzenta, 2006):

$$kL = \sqrt{\frac{\pi f}{a}}\,L = \sqrt{\frac{\pi}{a\,\tau_\Omega}}L > K_{\min}\,. \tag{17}$$

The value of $K_{\min}$ for 2% and 1% discrepancy was stated at $K_{\min\,1\%} = 1.78$ and $K_{\min\,2\%} = 2.25$ respectively (Panas & Nowakowski, 2009). The discrepancy concerns the relative difference between the approximate thermal diffusivity value a_ψ or a_φ derived from Eqs. (16) in relation to the appropriate value obtained from Eqs. (15).

Analysis of linear components of the excitation and the response provides additional opportunity for the thermal diffusivity evaluation from the time $\Delta\tau$ or the temperature lag ΔT (comp. Fig. 2). The procedure is equivalent to application of 2nd kind regular heating regime methodology (Volokhov & Kasperovich, 1984). Directly from Eq. (12) one gets

$$a = \frac{b\left(x^2 - L^2\right)}{2\Delta T} = \frac{x^2 - L^2}{2\Delta\tau} \;\wedge\; x = 0 \qquad \Rightarrow \qquad a = \frac{-bL^2}{2\Delta T} = \frac{-L^2}{2\Delta\tau}\,. \tag{18}$$

The major advantage from imposing a linear scan is that the temperature function of the thermal diffusivity can be obtained within one continuous experiment without necessity for successive changing and stabilizing the sample temperature. However, it should be underlined that the investigation needs to be planned and performed with a special care in view of the assumption concerning linearity of the problem. This can be done preserving the appropriate thermal/temperature resolution of the experiment (see eg. Panas, 2010).

2.3 Generalized model for the 1st kind regime of monotonic heating of a slab

Mathematical formulation of this heat conduction problem requires , as in the previous case, putting ν=0 into the governing Eq. (1). The problem is formulated for the interval $0 \le x \le L$, applying homogeneous initial temperature distribution $\theta(x,0) = 0, \quad 0 \le x \le L$. For the BC the following expressions apply:

$$\frac{\partial \theta(0,\tau)}{\partial x} = 0, \quad \frac{\partial \theta(L,\tau)}{\partial x} = \frac{H}{\lambda}\left\{\theta_D\left[1 - \exp\left(-\frac{\tau}{\tau_{ch}}\right)\right] - \theta(L,\tau)\right\}. \tag{19}$$

where τ_{ch} is the (characteristic) time constant of exponential surface treatment. For $\tau_{ch} \to \infty$ we get an asymptotic approximation of classical step heating function (comp. Volokhov & Kaperovich, 1984). The solution is given by (Lykov, 1967):

$$\theta(x,\tau) = 1 - \frac{\cos\dfrac{x}{\sqrt{a\tau_{ch}}}}{\cos\dfrac{L}{\sqrt{a\tau_{ch}}} - \dfrac{\lambda}{H\sqrt{a\tau_{ch}}}\sin\dfrac{L}{\sqrt{a\tau_{ch}}}}\exp\left(-\frac{\tau}{\tau_{ch}}\right) - \sum_{n=1}^{\infty}\frac{A_n \cos\dfrac{\mu_n x}{L}}{1 - \dfrac{a\tau_{ch}\mu_n^2}{L^2}}\exp\left(-\mu_n^2\frac{a\tau}{L^2}\right), \tag{20}$$

where μ_n are roots of

$$\tan\mu = -\frac{\mu}{\mathrm{Bi} - 1}, \quad \mathrm{Bi} = \frac{HL}{\lambda}, \tag{21}$$

and constants A_n are given by

$$A_n = (-1)^{n+1}\frac{2\mathrm{Bi}\sqrt{\mu_n^2 + (\mathrm{Bi} - 1)^2}}{\mu_n^2 + \mathrm{Bi}^2 - \mathrm{Bi}}. \tag{22}$$

The above presented model has been included into consideration mostly for comparison reasons and because of the needs for referring to some previous results of TP investigation applying IR imaging technique. Analysing the result given by Eq. (20) one can notice that, similarly as in the previous cases, a long term approximation can also be derived by neglecting all but the first one (n=1) series components. However, this solution does not describe a developed (stabilised) thermodynamic process of a finite "amplitude"[1]. It results in lowering values of sensitivity coefficients[2] with increasing time when the temperature of the body equilibrates.

2.4 Comments on the implementation of the TD measurement procedure applying IR imaging technique

There are two basic prerequisites for a successful implementation of a certain heat transfer model for TP/TD investigation. The first is precise reconstruction of all the model

[1] It can be the amplitude, the time lag or the temperature lag as shown in Fig. 2.
[2] For more detailed description of the sensitivity issue see Özişik & Orlando, 2000.

assumptions in the performed experiment. The second is that the heat flow should not be affected by the measurement procedure.

Implementation of the infrared imaging technique creates unique opportunity for non-intrusive analyses of the temperature distribution and its evolution in time. However, in many cases these studies are limited to qualitative studies. Investigations of the hard tooth tissues performed by Sakagumi & Kubo, 2002 or by Panas at all., 2007 can serve as an example of that. The major problems arise from not so good performance in quantitative measurements of the absolute temperature. The measurements are strongly dependent on the surface condition and influenced by surroundings. Usually precise estimation of the surface emissivity, which is the crucial parameter for the temperature assessment, could be problematic. For this reason, investigations are frequently planned to account for the temperature differences or for the temperature evolution only. Cooling fin (Miettinen at all., 2008; Rémy at all., 2005), cooling block (Perkowski, 2011) or flash experiments (Bison at all., 2002) can serve as typical examples of that. The temperature oscillation technique exhibits a unique performance in that domain. Being not dependent on the absolute temperature measurements, it reduces major IR technique implementation problems. The TD investigation procedure is based on the amplitude ratio and on the phase lag evaluation. This is why we notice a growing popularity of this methodology both in qualitative and in quantitative investigations (see eg. Bison et all., 2002; Muscio at all., 2004).

Performing measurements one still should take into consideration increased heat losses from the IR monitored surface. These losses can affect the applied theoretical model conformity. The investigated object needs also to be separated from the surrounding irradiation. If the above mentioned problems cannot be avoided while performing the experiment they need to be corrected applying other techniques and/or accounted for in the course of the uncertainty budget analysis.

3. Experimental

Developing an experimental system for the TD investigation at different heating modes one should keep in mind the limitations imposed by the applied mathematical models. However, even in this case the system can be adapted for multi-mode operation. Such versatility is not only economically reasonable but is judicious from metrological point of view. By comparing the data from different experiments the appropriate procedures can be tested and the experimental results can be verified. Of course, the experiment management and data processing procedures should be also accommodated. Realization of this concept for the 1st, 2nd and 3rd kind of regular heating regime TP investigation is described below.

3.1 Experimental setup

The actual experimental system configuration depends on the type of the investigated specimen. There are two basic modes of the system operation: for measuring in-plane (longitudinal) TD of bars, plates and sheets/foils (Fig. 3.a,b,c) and for transversal TD measurement of plates (Fig. 3.d). The in-plane measurements are further differentiated respecting the investigated material anisotropy to ensure effective heat transfer into the body of the sample (see Fig. 3.c). The specimen is usually pressed between two thermoelectric Peltier elements or pressed to the elements' unipolar side surface. If necessary, thermally

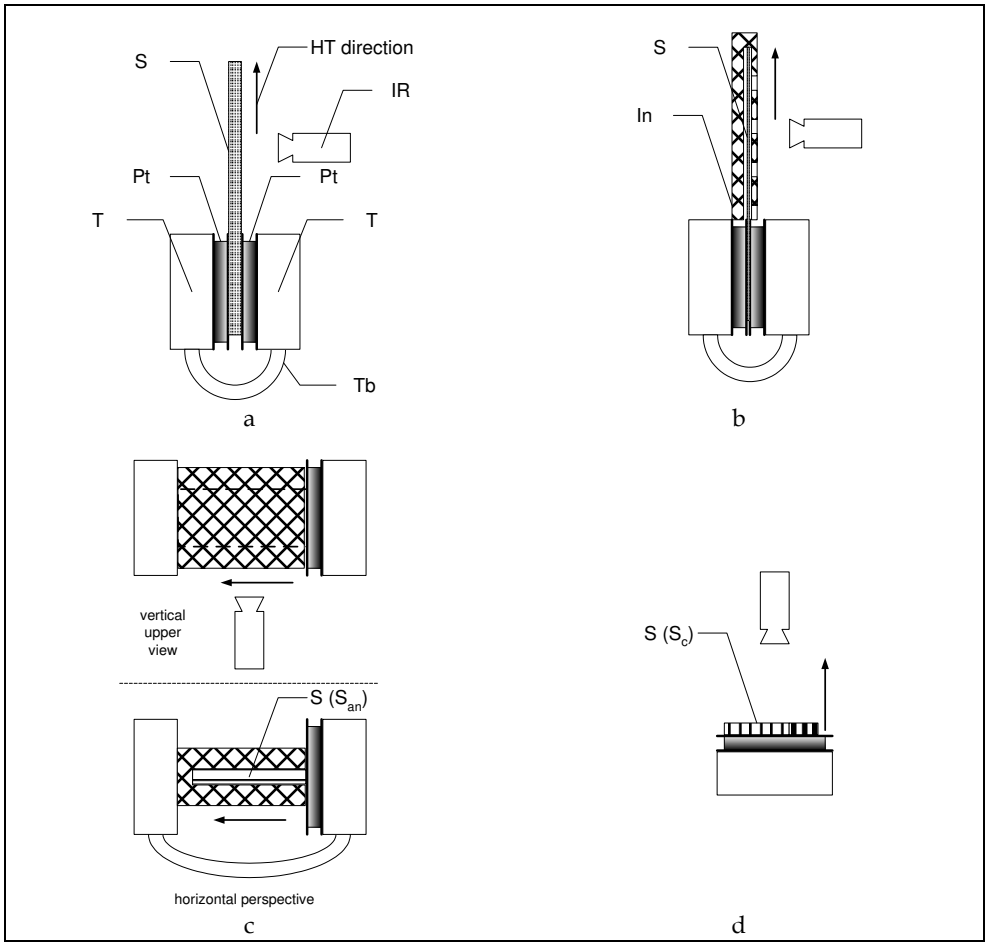

Fig. 3. Typical arrangements of longitudinal TD measurement applying an IR camera for: a – slabs, b – thin sheets and foils and c- bars of anisotropic materials, d - for transversal TD investigation of slabs/composite slabs (d); S – specimen, S_{an} – anisotropic specimen, S_c – composite non-homogeneous specimen, HT – heat transfer direction, Pt – Peltier thermoelectric device with the polarity indicated with shadowing, IR – infrared camera, T – thermostatic block, Tb – tubing, In - insulation

conductive paste is used to improve the thermal contact. Slab specimens of bad heat conductors studied for transversal TD are usually fastened with a thermal conductive resin or paste onto an additional conductive plate (usually made of copper). This is to homogenize the lateral temperature distribution. The periodic or exponential boundary excitation is performed by the appropriate powering of Peltier elements. As it is shown in Fig. 4 thermoelectric elements are powered by a DC power supply (Amrel PPS 1320). In typical measurements the power supply voltage is changed every 1 s to accommodate the demanded power changes according to the following formulae:

$$U(\tau) = U_0 + U_A(1+\sin\omega\tau) \quad \vee \quad U(\tau) = \begin{cases} 0 & \tau < 0 \\ U_A(1-\delta\, e^{-\frac{\tau}{\gamma}}) & \tau \geq 0 \end{cases}, \tag{23}$$

where U_A is the amplitude, U_0 - offset voltage (that can be changed programmatically), δ=0 or 1, and γ is the appropriate time constant. The temperature of every Peltier element opposite end is stabilized by thermostatic blocks fed from a thermostat (Lauda RL6CP). The Lauda device can operate in a programmable mode. This option is applied to ensure a linear change of the oscillation offset. The time-dependent temperature field in the sample is recorded with an infrared camera (Flir SC5600) and stored into the PC memory. The specimen attached to the heating (cooling) unit is separated from enviroment by an illumination protective shield that simultaneously fulfils the role of a thermal insulating guard. The instrumentation is supplemented by an 8 channel temperature recorder (NI SCXI 1000 system). The additional measurements of the temperature are made for control and verification purposes and are performed with thermocouples. The whole system is controlled from the PC through GPIB (SCXI), Fast Ethernet (IR camera) and RS232 (Lauda) buses. For this function special virtual instrumentation software has been implemented.

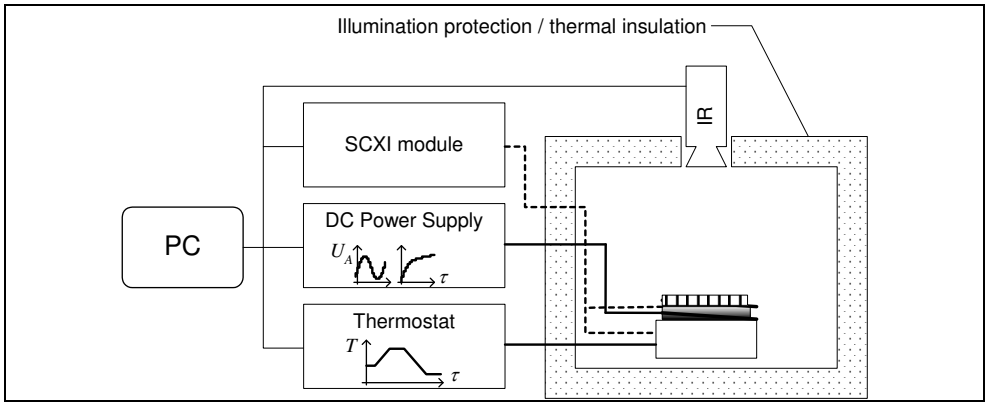

Fig. 4. Schematic diagram of the experimental setup for thermal diffusivity measurements by temperature oscillation in scanning mode

3.2 Experimental procedures and data processing

Before mounting the specimens into the measuring unit, they are usually painted black with a Graphite 33 (Kontakt Chemie) graphite spray. The estimated thickness of the graphite layer is about 15 μm. The black layer is used to improve the surface emittance, homogenize surface emissivity and to prevent the recording from the effects of translucency (Fig. 5 - translucence effects are clearly seen at not painted strips). The effect of the graphite layer presence has been expected to be negligible because individual effects on the temperature excitation and temperature response compensate each other (see Eqs (7)).

During measurements the temperature of the thermostatic blocks is stabilized or being changed programmatically. In the case of step or exponential heating experiments, the whole process of the specimen temperature disturbance and stabilization is being recorded.

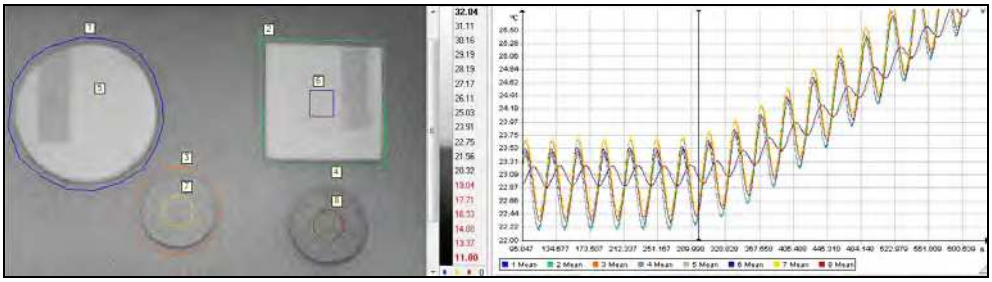

Fig. 5. Illustration of the IR data management: the IR image of polytetrafluoroethylene (PTFE; large disc), polymethylmethacrylate (PMMA; square) and two Al_2O_3-SiO_2 composite ceramic specimens during oscillation treatment (on the right) with a time history diagram of temperatures taken from selected lines (on the left)

While operating in the oscillation heating mode at least five to ten subsequent periods of the temperature change are recorded but usually the examination lasts much longer. The thermocouple temperature measurements are performed simultaneously with the IR camera recording. The sampling rates are adjusted to different study conditions.

At the end of measurements the time histories of the temperature/mean temperature taken from selected points, lines (see Fig. 5) or areas are processed with a specially developed software of a non-linear curve fitting. Prior to final calculation the aerial temperature data were inspected for any disruptions in uniform temperature distribution. The procedure of the step heating and exponential heating data approximation with a function:

$$f(\tau) = A_e \exp\left(-\frac{\tau}{B_e}\right) + C_e, \tag{24}$$

where A_e, B_e and C_e are the best fit coefficients, is similar to that described by Panas et al., 2005; 2007. The data from oscillation excitation experiments, are fitted with a function:

$$f(\tau) = A_s \sin(\omega\tau + B_s) + C_s + D_s\tau\,, \tag{25}$$

where A_s, B_s, C_s and D_s are the best fit coefficients. The constant D_s accounts for a linear component of the temperature changes. The approximate is usually obtained for every single "period". Next, the coefficients ψ and φ are calculated from the appropriate values of A_s and B_s of the two selected experimental time histories. Finally two complementary values of a_ψ and a_φ, are obtained by solving the Eq. (13). At this stage of calculation the appropriate distances or dimensions are being used. When Ångström's model assumptions apply, ie. in the case of a short "thermal wave" (comp. Carslaw & Jaeger, 2003), the appropriate amplitude a_ψ and phase a_φ TD values are calculated directly from Eq. (10) and the thermal diffusivity a is obtained from Eq. (9).

4. Typical results and discussion

The presented investigations have been selected mostly to illustrate typical experimental procedures and to show performance of the developed instrumentation and methodology.

The considered materials and structures are (Fig. 6): electrolytic pure copper [Cu], Ni_3Al nano-structural alloy [Ni3Al], anisotropic pyrolitic graphite [PG], polymethylmetacrylate [PMMA], polytetrafluoroethelene [PTFE] and sliced tooth structures (comp. Żmuda at all., 2005 and Panas at all., 2007). The Cu, PMMA and PTFE have been included mainly for testing and reference purposes. In all the cases the attention was focused on IR imaging methodology and such physical effects as anisotropy and non-homogeneity of the investigated specimens.

As was mentioned before, prior to the experiments the investigated structures had been coated as shown in Fig. 6 a, b and d. This did not concern the graphite specimen which did not need such treatment. During the measurements the temperature IR recordings were taken at stated sampling rates. Afterwards, the IR images were inspected for the temperature distribution non-homogeneity. Next, and the temperature histories were taken from previously selected objects/sections: point/spots, lines, segment lines, circle lines, circles or rectangular areas. The location of control sections is shown in Fig. 7.

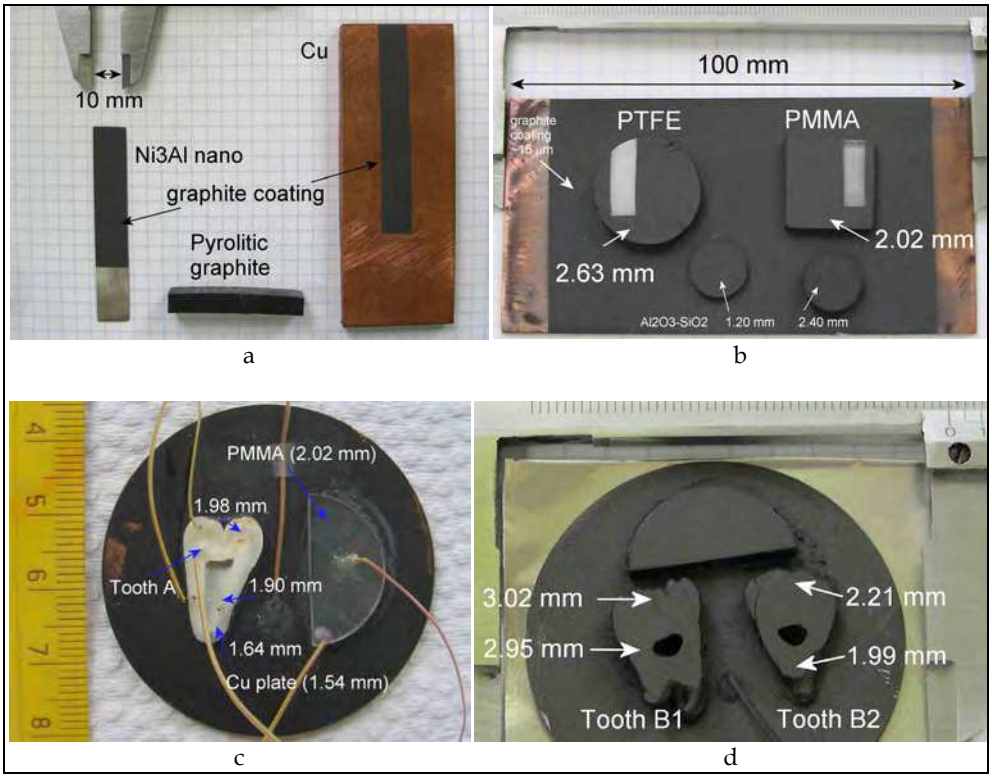

Fig. 6. Investigated specimens and structures: a – slabs (bars) of electrolytic pure copper (left), pyrolitic graphite (middle), and thin sheet of nano-structural Ni_3Al alloy studied for in-plane TD; b – plates of PMMA and PTFE; c – sliced tooth A with a reference PMMA half-disk just before applying a graphite layer, d – sliced tooth B structures coated with graphite. In the cases b, c, and d the specimens were investigated for their transversal TD.

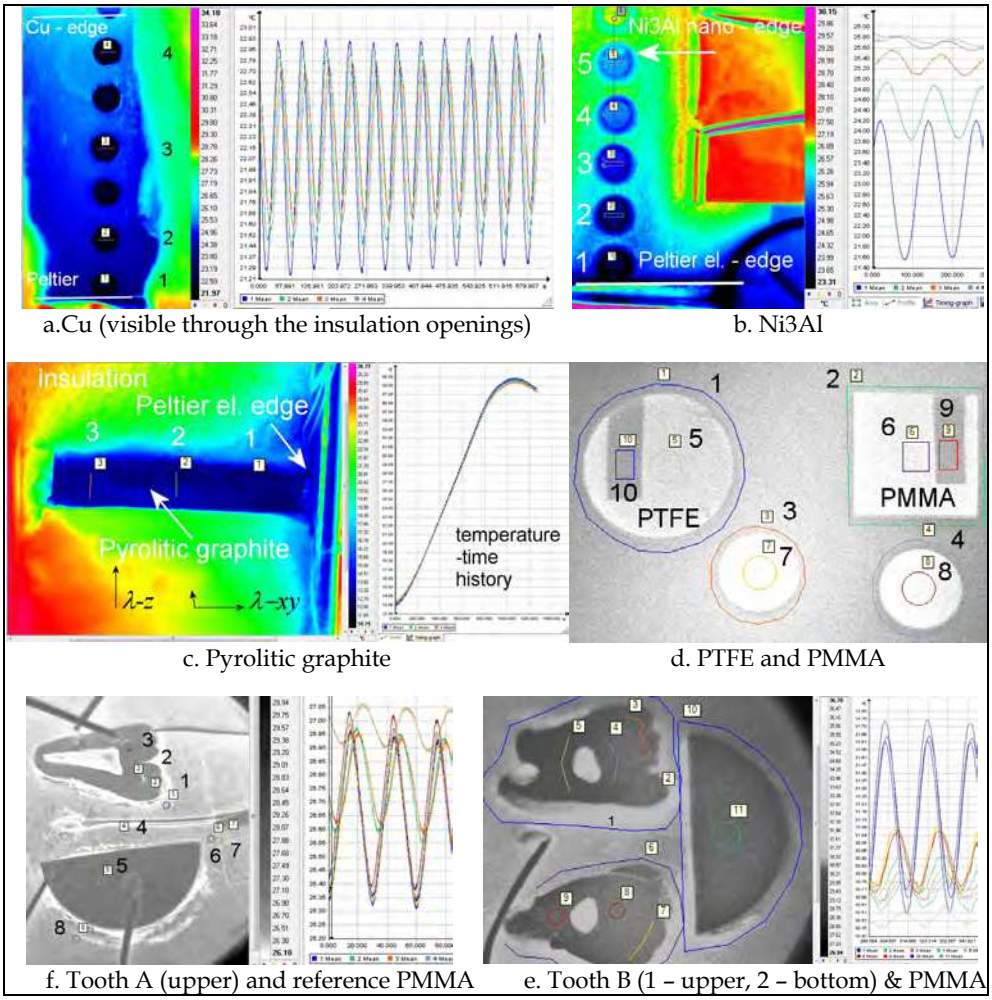

a.Cu (visible through the insulation openings) b. Ni3Al

c. Pyrolitic graphite d. PTFE and PMMA

f. Tooth A (upper) and reference PMMA e. Tooth B (1 – upper, 2 – bottom) & PMMA

Fig. 7. Illustration of the IR images of the investigated specimens with indication of control sections for the temperature history acquisition

4.1 Copper slab under long "thermal wave" treatment

The major problem with application of Ångström's method is to comply with the semi-infinite rod model. In practice it means that the investigated object should be long enough to damp down the temperature oscillations before reaching the far end of the specimen (Muscio at all., 2004; Phylippov, 1984). It makes the investigations of materials and objects which are available only in small pieces more difficult. This is the case of many advanced technology structures.

The measurements performed on a 100.0 mm × 38.0 mm × 5.80 mm slab of electrolytic pure copper were planned mostly to face this problem. They were carried out at sampling rate

equal to 2 Hz for the temperature oscillation over 22.2 °C with the period τ_Ω = 60 s. Application of long "thermal waves" not only violates the classical Ångström's assumptions but exceeds limits of conventional implementation of the modified method (comp. eg. Bodzenta at all., 2006). The parameter *kL*, defined by Eq. (15), amounted only to 0.42 that is much below the stated K_{min} limit for validity of simplified formulae given by Eq. (18). For that reason the data were processed utilising exact relations for a slab model given by Eq. (13).

Recordings of the specimen temperature were done through openings in the 5 mm thick polyurethane foam separating the Cu specimen from ambient air convection (Fig. 7.a). Twelve subsequent periods of temperature changes were recorded. The time curves for preparatory data processing - approximation according to Eq. (25) - came from lines *i* = 1, 2, 3 and 4 (Fig. 7.a). Next, the values

$$\psi_{ij} = \frac{A_{s,j}}{A_{s,i}}, \quad \varphi_{ij} = B_{s,j} - B_{s,i}, \quad T_{mean,ij} = \frac{C_i + C_j}{2} \quad , i > j, i = 1,2,3, \; j = 2,3,4 \, , \tag{26}$$

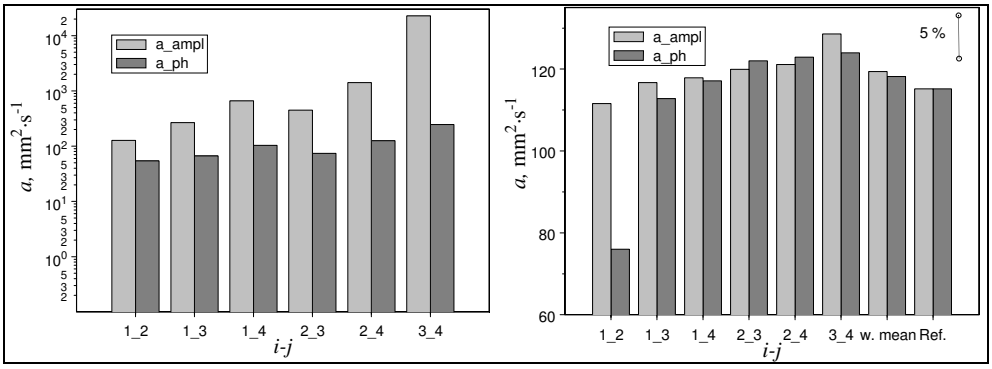

Fig. 8. Comparison of the apparent TD of Cu calculated from Ångström's formulae (9) – on the left – with values obtained by solving Eqs. (13) – on the right. The measurements were performed applying "long thermal wave" (at τ_Ω=60 s). The reference data is taken from Ražnievič, 1966.

were obtained from the approximation best fit parameters of corresponding single periods. This means that all possible mutual configurations of control lines were taken into consideration. Next, the appropriate: a_ψ - the amplitude and a_φ - phase values of apparent TD were derived by solving Eqs. (13) with

$$x = l = x_{ij} = \left| x_i - x_j \right|, \quad L = \left| x_{edge} - x_i \right| . \tag{27}$$

where x_i is a relevant control line coordinate and x_{edge} is the specimen free edge coordinate. It should be noticed that the same parameter l=x is applicable for classical Ångström's model data processing according to Eq. (9). Such processing was conducted in parallel calculations to provide illustrative comparable data. Finally, the obtained amplitude and phase TD values were averaged over all 12 periods of stable oscillations providing appropriately

$\overline{a}_{\psi,ij}$ and $\overline{a}_{\phi,ij}$ mean values. The time averaged data are shown in Fig. 8 for both models: the semi-infinite rod (on the left) and the slab (on the right). With no doubt the "classical" results are unacceptable which was expected regarding the applied long "thermal wave" excitation. The quality of these results worsens while approaching the specimen free edge. On the contrary, the modified procedure results are in a good agreement with the reference data taken from Ražnievič, 1966. The results of comparison are even better when the following weighted mean value

$$\overline{a}_{w\_mean} = \sum_{i=1}^{M-1}\sum_{j=i+1}^{M}\left(x_i - x_j\right)^2 \overline{a}_{ij} \Bigg/ \sum_{i=1}^{M-1}\sum_{j=i+1}^{M}\left(x_i - x_j\right)^2 , \tag{28}$$

is considered. In Eq. (28) the M stands for a total number of subsequent control sections – in the present case M=4. The weights, in a form of squared distances, account for dimensional dependence of the calculated TD. The obtained $\overline{a}_{\psi,w\_mean}$ and $\overline{a}_{\varphi,w\_mean}$ values are shown in Table 1. The discrepancy between global weighted mean values and the reference data is not greater than 3.7%.

Analysing the individual data one can even identify some specific effects like nonconformity with one-dimensional model assumptions. This is the most probable reason for underestimation of $\overline{a}_{\psi,12}$ and $\overline{a}_{\varphi,12}$ results.

Concluding, it should be pointed out that the experiment has proved a good metrological conditioning of the temperature oscillation technique combined with the IR imaging technology.

i-j	1-2	1-3	1-4	2-3	2-4	3-4	w. mean	Ref.
l , mm	9.78	29.21	49.65	19.43	39.87	20.44	n.a.	n.a.
a_ψ, mm²·s⁻¹	111.6	116.7	117.9	119.9	121.1	128.6	119.4	115.2
a_φ, mm²·s⁻¹	76.0	112.8	117.1	122.0	122.9	123.9	118.2	

Table 1. Results of electrolytic pure copper TD investigation with modified Ångström's procedure compared with the reference data according to Ražnievič, 1966

4.2 Nano-structural Ni3Al intermetallic alloy

The major challenge of the TD investigation of intermetallic Ni_3Al alloy is that the nanostructural material is available only in the form of thin metallic sheets. In such a situation the non-intrusive character of the IR temperature measurements is essentially beneficial (comp. Nakamura, 2009). However, it should be underlined that infrared measurements can be effectively performed only in a narrow range of temperature changes.

The procedure that was tested on Cu specimen has also been applied for a Ni_3Al alloy investigation. The specimen was delivered in the form of a sheet 0.63 mm thick, 11.00 mm wide and about 66 mm long (Fig. 6.a – on the left). The measurements were carried out at sampling rate equal to 1 Hz for the temperature oscillation over 23 °C with the period τ_Ω = 120 s (Fig. 7.b). The obtained results are shown in Fig. 9 and displayed in Table 2. They were supplemented with one more parameter that is a geometric mean of the amplitude and phase apparent TD values:

$$a_{g\,mean} = \sqrt{a_\psi \, a_\varphi} \quad , \tag{29}$$

The discrepancy between a_ψ and a_φ can be attributed to heat losses from the specimen. Taking into account relatively high ratio of the specimen perimeter p to its cross-section area S, they are extremely influential. The heat losses resulted in a high ν parameter value (comp. Eq. 3), but they are not considered in a slab model. However, regarding the expected asymptotic convergence of the appropriate solutions when increasing the L parameter of a slab model one can assume that a_ψ is the underestimate and a_φ is the overestimate of the real TD value as in the case of semi-infinite rod (comp. Eqs. 6, 9 and 10). This was confirmed in the course of numerical simulation. Moreover, it was stated that the geometric mean value defined by Eq. (29) is a good approximation of the real TD value for certain parameters of combined conductive and convective heat losses. The detailed discussion is outside the scope of this review so we restrain to this communication only.

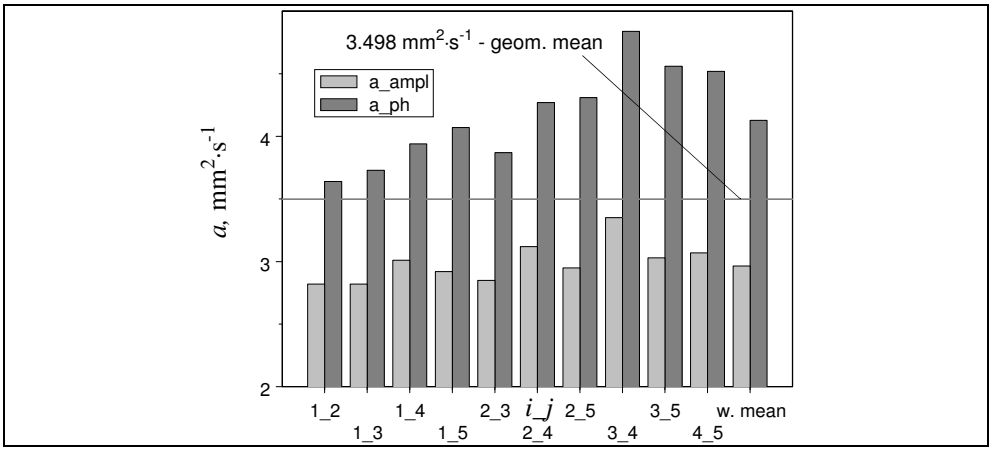

Fig. 9. Results of TD investigation of Ni_3Al nanostructural intermetallic alloy

i-j	1-2	1-3	1-4	1-5	2-3	2-4	2-5	3-4	3-5	4-5	w.mean	g.mean
l , mm	9.90	19.98	29.47	39.72	10.08	19.57	29.82	9.49	19.75	10.25	n.a.	n.a.
a_ψ, mm²·s⁻¹	2.82	2.182	3.01	2.92	2.85	3.12	2.95	3.35	3.03	3.07	2.964	3.498
a_φ, mm²·s⁻¹	3.64	3.73	3.94	4.07	3.87	4.27	4.31	4.84	4.56	4.52	4.128	

Table 2. Results of TD studies of Ni_3Al nano-structural intermetallic alloy specimen

4.3 Pyrolitic graphite

Pyrolitic graphite (PG) is one of a few commercially available highly anisotropic materials. Typically, its in-plane thermal conductivity λ_{xy} exceeds transversal (out-of plane) λ_z value for at least two ranges (comp. Heusch at all., 2002). The same concerns also thermal diffusivity. Because of that the PG specimen was investigated applying the system arrangement as shown in Fig. 3.c. The in-plane dimensions of the specimen were 44.0 mm and 9.6 mm for x and y direction respectively. Transversally the investigated bar was 6.5

mm thick. The measurements were performed at 2 Hz sampling rate for the temperature oscillation period $\tau_\Omega = 10$ s. The offset temperature was quasi-linearly changed within the interval from about 12°C to 38 °C (Fig. 7.c). The results of measurements are shown in Fig. 10. Contrary to three previously discussed cases, the obtained data have not been averaged. Instead of that, linear regressions were derived for both the amplitude and phase apparent TD. The appropriate coefficients are given in Table 3.

In spite of a relatively high scatter of individual data the discrepancy between a_ψ and a_φ characteristics is not so significant. It is because of a relatively small τ_Ω value which is the major cause of the scatter. But proving the effectiveness of modified linear scanning procedure was the most important outcome of the investigation (Panas & Nowakowski, 2009).

Regarding the quantitative aspect of the results it should be noticed that they exceed those reported by Maglić & Milošević, 2004 by about 2.5 times and are at least 8 times lower than presented by Heusch at all., 2002. This is not a surprise considering the differences of PG manufacturing technology. The tendency of the TD changes is exactly as expected: it decreases with the increasing temperature.

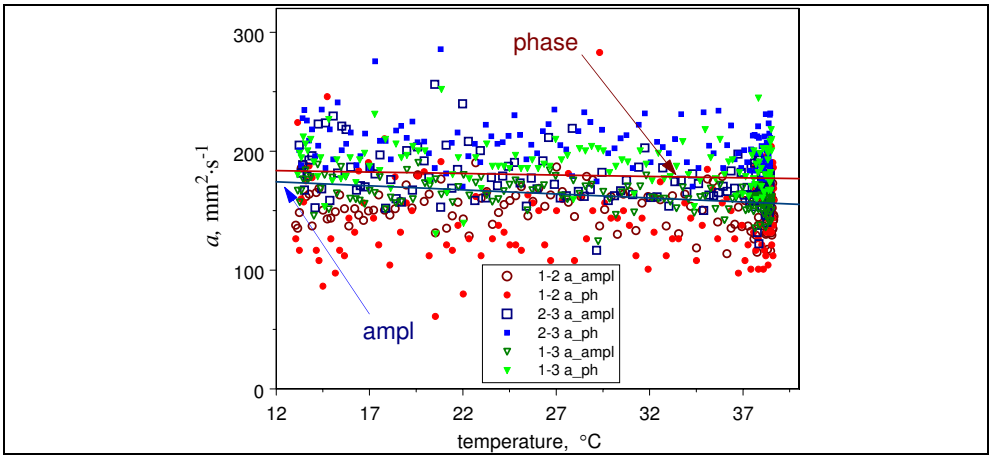

Fig. 10. Results of investigation of the TD temperature dependence of pyrolitic graphite

a_ψ, mm²·s⁻¹	182.4640 - 0.6800363 ·t/°C	13 °C ≤ t ≤ 38 °C
a_φ, mm²·s⁻¹	186.5935 - 0.2439950·t/°C	

Table 3. Linear regressions for pyrolitic graphite TD (t – temperature in °C)

4.4 PMMA and PTFE slabs

The aim of this part of research was to test and to verify procedures for investigation of transversal TD of slabs. The PMMA and PTFE were selected because literature data on their properties are easily available (Panas at all., 2003b; Tye & Salmon, 2005; Blumm at all., 2010). The experiments were conducted in the system configuration as shown in Fig. 3.d. The

investigated specimens are shown in Fig. 6.b. All measurements were performed at 2 Hz sampling rate for the temperature oscillation period $\tau_\Omega = 30$ s. They started from steady oscillations over 22.5 °C. Next, the temperature scan from this temperature up to 41 °C was added (Fig. 5). Because one of the studied phenomena was the specimen transparency effect, each time the temperature response was taken from both the graphite coated part of the upper specimen surface and from the area intentionally left free from the coating. For the temperature data collection rectangular areas were applied as shown in Fig. 6.d (see also Figs 5 and 7.d). The signals were compared with the temperature histories taken from a semi–circled segment line around the PTFE and tetragonal line around the PMMA specimen respectively. The a_ψ and a_φ were obtained by solving Eqs (15). The final results are shown in Fig. 11. The data from the steady offset part of experiments is also listed in Table 4. They prove correctness of the applied procedure and show the translucence effect. It should be mentioned that routines of a specimen layering are applied also when investigating TD by any other method involving radiation (see eg. Blumm at all., 2010; Kim & Kim, 2009; Panas at all., 2003; Maglić at all., 1984). The scanning measurements have revealed increasing data scattering that can be attributed to raised convection (Fig. 11.b). This is why wide temperature range measurements of slab specimens become more difficult. Regarding such investigations it should be

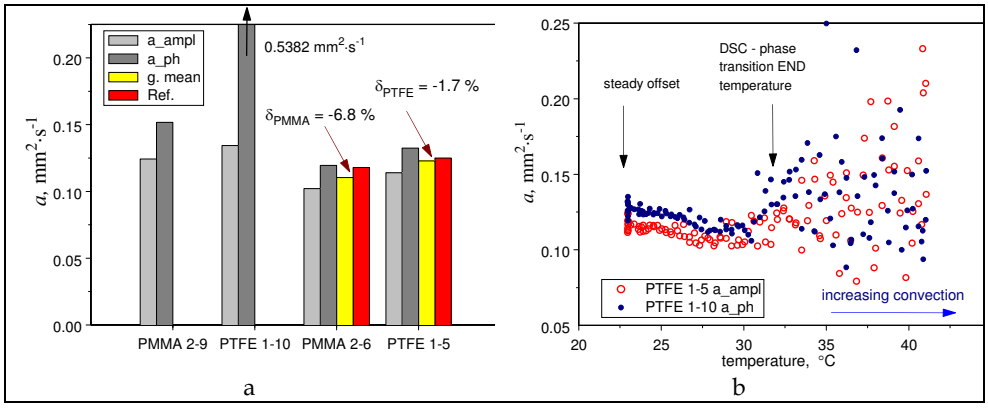

Fig. 11. Results of PMMA and PTFE investigation: a - amplitude and phase apparent TD values from uncoated (2-9 and 1-10) and graphite coated areas (2-6 and 1-5) and their respective geometric means (Eq. 29) compared with the reference data from Salmon & Tye, 2005 and Blum at all., 2010; b – PTFE apparent TD dependence on the temperature (scanning step results; DSC END temp. – from Panas at all., 2003)

Data on:	PMMA				PTFE			
	uncoated	coated	g. mean	Salmon & Tye, 2005	uncoated	coated	g. mean	Blumm at all., 2010
a_ψ, mm²·s⁻¹	0.1243	0.1021	0.1104	0.1179	0.1343	0.1140	0.1229	0.1250*
a_φ, mm²·s⁻¹	0.1518	0.1195			0.5382	0.1325		

Table 4. Results of TD studies of PMMA and PTFE at 22.5 °C compared with literature data (*) - the result was interpolated from results by Blumm at all., 2010)

underlined that the other basic restrictions originate from the IR camera calibration. Nevertheless, the obtained characteristics enable to reveal the phase change effect that is in agreement with previously published data (Blumm at all., 2010; Panas at all., 2003).

4.5 Hard tooth structures – Temperature oscillation treatment

The hard tooth tissue investigation is a crucial one regarding the fact that the described IR "slab" technology is dedicated mostly to such problems. The measurements were performed on test specimens that had been previously studied both applying the IR camera (Panas at all., 2007) and thermocouples. In present investigation a close-up view (Fig. 7.e, f) recordings were taken at 10 Hz sampling rate for specimen A and 2 Hz sampling rate for specimen B1/B2 (see Fig. 6.c,d). The temperature oscillation period was 20 s and steady offsets were 26.7 °C and 31.2 °C for specimens A and B respectively. The temperature signals taken from control sections (Fig. 7. E,f) were processed the same way as discussed in the previous section. The results are shown in Fig. 12.

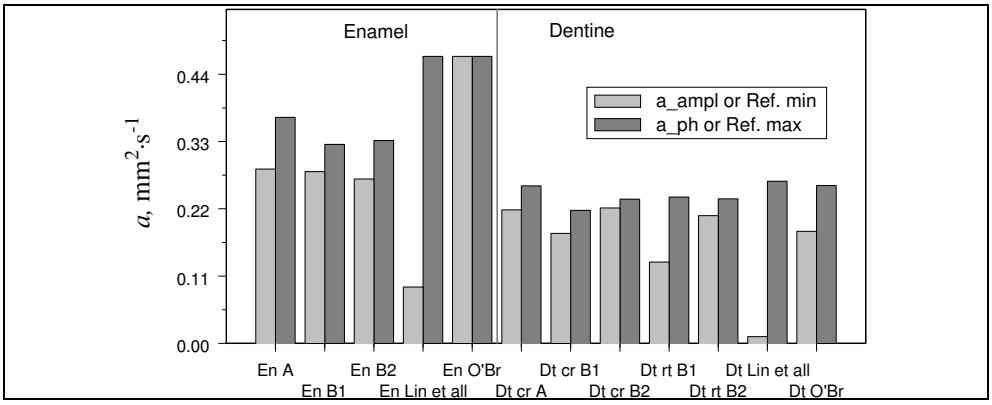

Fig. 12. Results from hard tooth structure TD studies: En indicates enamel, Dt cr – crown dentine, Dt rt – root dentine. The reference min/max data come from O'Brien, 1997 and Lin at all., 2010.a.

Analysing the displayed data one can notice that general relation between the enamel and dentine TD reported in the literature is properly expressed. The obtained ratio of enamel to dentine diffusivity is about 1.5. Moreover, the dentine results agree with most of the previously published data (comp. O'Brien, 1997; Panas at all, 2003, Lin at all., 2010a, 2010b). Considering the enamel data reported by Lin at all., 2010b and by O'Brien, 1997 the present enamel results might be regarded as underestimated. To express the differences more clearly geometric means (Eq. 29) from individual results were calculated first and next the data were averaged over similar characteristic tooth structures. These results are displayed in Table. 5.

In general, the problem of hard tooth tissue thermal properties is still open (comp. eg. Lin at all, 2010a). Taking this into account the obtained results can be regarded as acceptable. In spite of the fact that three different specimens from two different teeth were investigated, the obtained data are in mutual agreement. For that reason we can assume that the IR supported methodology of oscillating heating investigation of such objects is correct.

	Thermal diffusivity, $mm^2 \cdot s^{-1}$		
	Enamel	Dentine (crown)	Dentine (root)
$a_{A,B1,B2}$ (mean)	0.308	0.221	0.200
O'Brien at all., 1997	0.469	0.183 ÷ 0.258	
Lin at all., 2010b	0.408 (±0.0178)	0.201 (±0.05)	

Table 5. Results of TD studies of PMMA and PTFE at 22.5 °C compared with literature data (*) - the result was interpolated from results by Blumm at all., 2010)

4.6 Hard tooth structures – Step heating experiments

There are few reports on successful implementation of the step heating procedure in quantitative analyses of thermophysical properties of thin non-homogeneous slabs. Such a paper has been recently published by Lin at all., 2010. It presents the results of hard tooth tissue TD measurements and these data have been taken as one of the references in the previous section. However, to obtain quantitative results the researchers were forced to apply a special data processing. More often the analyses are limited to qualitative studies (Panas at all., 2007; 2003a). It is because the step heating boundary condition is difficult to apply. As an illustration of the problem the results of investigation described by Panas at all., 2007 can be indicated. The study was conducted with almost the same arrangement of the system as depicted in Fig. 4 except that Peltier elements had not been present. Tooth specimens B1 and B2 were heated through the copper plate by a sudden flow of water beneath. The temperature histories were taken from points located as indicated in Fig. 13.a. The obtained relative temperature differences $\Delta t = t_{Cu} - t_i$, $i = 1, \ldots, 5$ are shown in Fig. 13.b. As was expected the qualitative differences are easy to recognize. It does not concern quantitative analyses.

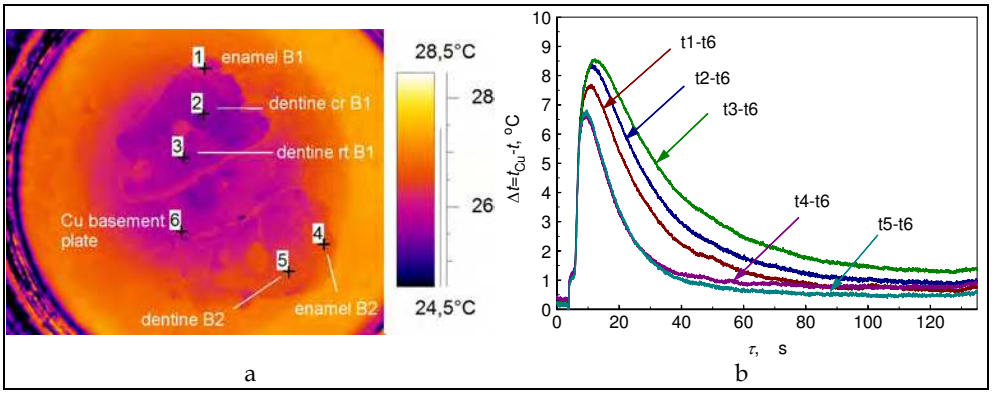

Fig. 13. The specimens B1 and B2 under monotonic heating (a; Panas at all., 2007)) and the temperature changes with reference to the copper plate temperature (b)

To examine the problem let us consider the model of the temperature evolution given by Eq. (20). Assuming perfect surface conductance ($Bi = \infty$) we get from Eqs. (20)-(22):

$$\theta(0,\tau)-\theta(L,\tau)=\left[1-\left(\cos\frac{L}{\sqrt{a\tau_{ch}}}\right)^{-1}\right]\exp\left(-\frac{\tau}{\tau_{ch}}\right)+\sum_{n=1}^{\infty}\frac{2(-1)^{n+1}}{1-a\tau_{ch}\pi^2n^2L^{-2}}\exp\left(-\pi^2n^2\frac{a\tau}{L^2}\right). \quad (30)$$

As we can see, the procedure of single exponential approximation (24) do not comply with the model formulae (30). The "amplitude" of the first exponential term is depended on a and this makes any modification more difficult. Application of Eq. (24) is limited to qualitative analyses (Panas at all., 2007). Only when $\tau_{ch} \to 0$ the TD identification can be done more easily. This is not the case regarding the discussed experimental results.

5. Numerical validation of TD investigation procedures

In comparison with standard procedures the IR imaging techniques are usually more demanding when applied to thermophysical property quantitative investigation. It is because of their increased sensitivity to environmental influences. The environment is also a source of major incompatibilities between the applied mathematical model and real experimental conditions. It was proved that analytical approach in the studies where such discrepancies appear is ineffective in most of the cases. For that reason, the investigation procedures are tested, validated and corrected in the course of numerical simulations. This is also the case in the studies described above. Because a detailed discussion on numerical modelling issue is outside the scope of this work, only a short review of selected results will be provided here.

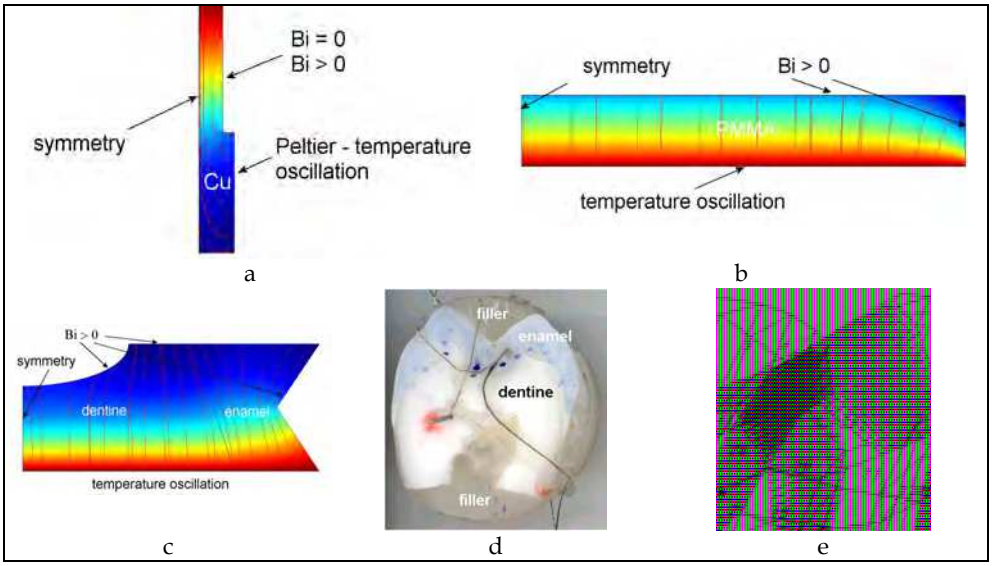

Fig. 14. Illustration of selected analysed numerical models: a – model for investigation of non-unidirectional heat transfer in Cu specimen, b – studies of convective heat losses from a slab specimen, c – 2D model for investigation of effects of non-homogeneity of a tooth specimen under periodic heating, d and e – the modelled structure and 3D model for investigation of laser flash and monotonic heating experiments of hard tooth tissues (Żmuda at all., 2005).

The numerical analyses were focused mostly on such problems as non-unidirectional heat transfer (Fig.14a), convection heat losses that violate assumptions of a slab model (Fig. 14.b), irregularity and non-homogeneity of the investigated tooth structure (Fig. 14.c) and 3D heat transfer effects including incompatibility of the temperature excitation (Fig. 14.d and e; see also Żmuda at all., 2005). In all the instances the elaborated models were also tested for the scanning mode application (comp. Panas & Nowakowski, 2009). The major outcome of these studies is the proof of correctness of the developed procedures for experimental TD investigation. The analyses proved good metrological conditioning of the oscillation technique. This concerns also the scanning mode operation.

Moving to the details, effects of 3D heat transfer in a laterally heated Cu specimen were confirmed (see red streamlines marking total heat flux path in Fig. 14.a). It was observed that both convective and conductive heat losses from side surfaces of slab specimens result in underestimation of amplitude and overestimation of phase results. This is similar to Ångström's model for semi-infinite rod. In the study of hard tooth tissue non-homogeneity effects, significant underestimation of the enamel results was revealed. This concerns not only the "thermal wave" measurements but also pulse heating experiments and monotonic heating investigations (Żmuda at all., 2005). The identified TD values were about 20% lower than that assumed in the model. The simulations showed that there is an influence of the control area location on the obtained enamel parameters. Because of this outcome, IR measurements seem to be more advantageous than traditional techniques that exclude monitoring of spatial temperature distribution.

It should also be mentioned that the numerical simulation technique has been applied for validation of the methodology for investigation of metallic specimens covered with a graphite layer. This concerns Cu and Ni3Al specimen studies. In both cases the effect of the covering has been proved to be negligible. However, in order to get more universal results a more thorough analyses needs to be performed like those concerning laser flash technology (comp. Cernuschi at al., 2002, S.K. Kim & Y.-J. Kim, 2009).

In general, a numerical modelling technique has not only proved to be helpful but also indispensable for discussed tasks. The only problem is that complicated objects need to be treated individually.

6. Conclusion

With its possibility of non-intrusive and simultaneous examination of both the temperature changes in time and temperature spatial distribution the IR imaging technology creates unique possibilities for complex thermal investigations. For that reason it is widely applied eg. in non destructive testing. However, application of IR imaging is restricted mostly to qualitative analyses because of its limitations. This applies also to thermophysical property investigation. In that domain the major disadvantages are related to: difficulties in complying with certain analytical model assumptions; narrow temperature range of operation when compared with standard techniques of TP studies (comp. eg. Maglić at all., 1984); unreliable temperature measurements due to the surface emissivity changes etc. On the other hand, the standard procedures of thermophysical property investigation are demanding for the investigated specimen structures and forms. This concerns mostly heat transfer parameters including the thermal diffusivity. In such a

situation the IR imaging technology seems to be indispensable especially when materials possessing unusual properties, exhibiting complicated structure or non-homogeneous composition are tested. As it has been shown in the present study reliable quantitative results of the thermal diffusivity investigation can be obtained providing that the IR technique is combined with a properly selected thermal treatment methodology. Regarding the problem of the temperature field excitation, the temperature oscillation proved to be well metrologically conditioned. This enabled accommodating the classical and modified Ångström's procedures (Ångström, 1961; Bodzenta at all., 2007) to the scanning mode operation (Panas & Nowakowski, 2009). These techniques combined with IR measurements of the spatial and temporal temperature changes enable successful investigations of the thermal diffusivity of "difficult" specimens. Measurements of pyrolitic graphite, nanostructural Ni_3Al intermetallic and hard tooth tissue structures illustrate good performance of that methodology. With no doubt, measurements performed on biological specimens are the most demanding. Because of that the results of these studies should be additionally verified. Numerical simulation proves to be the most effective technique for this task.

7. Acknowledgment

The experimental instrumentation of the research was completed with a support from UE/state POIG.02.02.00-14-022/09 project.

8. References

Ångström, A. J. (1861). Neue Methode, das Warmeleitungsvermogen der Korper zu Bestimmen. *Annalen der Physic und Chemie*, Vol. 114, (1861), pp. 513-530

Belling, J.M. & Unsworth, J. (1987). Modified Ångström's method for measurement of thermal diffusivity of materials with low conductivity. *Review of Scientific Instruments,* Vol.58, No.6, (June 1987), pp. 997-1002, ISSN 0034-6748

Bodzenta, J.; Burak, B.; Nowak, M.; Pyka, M.; Szałajko, M. & Tanasiewicz, M. (2006). Measurement of the thermal diffusivity of dental filling materials using modified Ångström's method, *Dental Materials*, Vol.22, No. , (July 2006), pp. 617–621, ISSN 0 109-5641

Bison, P.G.; Marinetti, S.; Mazzoldi, A.; Grinzato, E. & Bressan, C. (2002). Crosscomparison of thermal diffusivity measurements by thermal methods. *Infrared Physics and Technology*, Vol.43, No.3–5 (June 2002), pp.127–132, ISSN 1350-4490

Blumm, J.; Lindemann, A., Meyer, M. & Strasser, C. (2010). Characterization of PTFE Using Advanced Thermal Analysis Techniques. *International Journal of Thermophysics*, Vol.31, No.1, (October 2010), pp. 1919-1927, ISSN 0198-925X

Carlaw, H. S. & Jaeger, J. C. (2003). *Conduction of Heat in Solids* (2nd Edition), Oxford Univ. Press, ISBN 978-0-19-853368-9, London, Great Britain

Cernuschi, F., Lorenzoni, L.; Bianchi, P. Figari, A. (2002). The effects of sample surface treatments on laser flash thermal diffusivity measurements. *Infrared Physics and Technology*, Vol.43, No.3–5 (June 2002), pp.133–138, ISSN 1350-4490

Heusch, C.A.; Moser, H.-G. & Kholodenko, A. (2002). Direct measurements of the conductivity of various pyrolytic graphite samples (PG, TPG) used as thermal

dissipation agents in detector applications. *Nuclear Instruments and Methods in Physics Research A*, Vol. 480, No.2-3 (March 2002), pp. 463-469, ISSN: 0168-9002

Kim, S.-K. & Kim, Y.-J. (2009). Determination of apparent thickness of graphite coating in flash method. *Thermochimica Acta,* Vol.468, No.1-2, (February 5, 2008), pp. 6-9, ISSN: 0040-6031

Lin, M.; Xu, F.; Lu, T.J. & Bai, B.F. (2010a). A review of heat transfer in human tooth—Experimental characterization and mathematical modeling. *Dental Materials*, Vol.26, No.6, (June 2010), pp. 501-513, ISSN: 0109-5641

Lin, M.; Liu, Q.D.; Kim, T.; Xu, F.; Bai, B.F. & Lu, T.J. (2010b). A new method for characterization of thermal properties of human enamel and dentine: Influence of microstructure. *Infrared Physics and Technology,* Vol.53, No.6, (November 2010), pp. 457-463, ISSN 1350-4490

Lykov, A.V. (1967). *Tieoria tieploprovodnosti*, Vysshaya Shkola, UDK-536.2, Moskva, USSR

Maglić, K. D.; Cezairliyan, A. & Peletsky, V. E. (Eds.). (1984). *Compendium of Thermophysical Property Measurement Methods. Volume 1: Survey of Measurement Techniques.* Plenum Press, ISBN 0-306-41424-4, New York, USA

Maglić, K. D.; Cezairliyan, A. & Peletsky, V. E. (Eds.). (1992). *Compendium of Thermophysical Property Measurement Methods. Volume 2: Recommended measurement Techniques and Practices.* Plenum Press, ISBN 0-306-43854-2, New York, USA

Maglić, K. D. & Milošević, N. D. (2004). Thermal Diffusivity Measurements of Thermographite. *International Journal of Thermophysics*, Vol.25, No.1, (January, 2004), pp. 237 – 247, ISSN 0198-925X

Miettinen, L.; Kekäläinen, P.; Merikoski, J.; Myllys, M. & Timonen, J. (2008). In-plane Thermal Diffusivity Measurement of Thin Samples Using a Transient Fin Model and Infrared Thermography. *International Journal of Thermophysics*, Vol.29, No.4, (August, 2008), pp. 1422 – 1438, ISSN 0198-925X

Muscio, A.; Bison, P.G.; Marinetti, S. & Grinzato, E. (2004). Thermal diffusivity in slabs using harmonic and one-dimentional propagation of thermal waves. *International Journal of Thermal Sciences*, Vol. 43, No.5 , (May 2004), pp. 453-463, ISSN 1290-0729

Nakamura, H. (2009). Frequency response and spatial resolution of a thin foil for heat transfer measurements using infrared thermography. *International Journal of Heat and Mass Transfer*, Vol.52, No.21-22, (October 2009), pp. 5040-5045, ISSN 0017-9310

O'Brien, W. J. (1997). *Dental Materials and Their Selection*, Quintessence Publ., ISBN 0-86715-297-4, Chicago, USA

Özişik, M.N. and Orlando, H.R.B. (2000). *Inverse Heat Transfer. Fundamentals and Application*, Taylor & Francis, ISBN 1-56032-838-X, New York, USA

Panas, A. J.; Żmuda, S.; Terpiłowski, J. & Preiskorn, M. (2003a). Investigation of the thermal diffusivity of human tooth hard tissue. *International Journal of Thermophysics*, Vol.24, No.3, (May 2003), pp. 837-848, ISSN 0198-925X

Panas, A.J.; Cudziło, S.; & Terpiłowski, J. (2003b). Investigation of thermophysical properties of metal-polytetrafluoroethylene pyrotechnic compositions. *High Temperatures - High Pressures*, Vol. 34, No.6 , (December 2003), pp. 691-698, ISSN 0018-1544

Panas, A.J.; Preiskorn, M.; Dąbrowski, M. & Żmuda, S. (2007). Validation of hard tooth tissue thermal diffusivity measurements applying an infrared camera. *Infrared Physics and Technology*, Vol.49, No.3, (January 2007), pp. 302-305, ISSN 1350-4490

Panas, A.J. & Nowakowski, M. (2009). Numerical validation of the scanning mode procedure of thermal diffusivity investigation applying temperature oscillation, *Proceedings of Thermophysics 2009*, pp.252-259, ISBN 978-80-214-3986-3, Valtice, 29th÷30th October 2009

Panas, A.J. (2010). Comparative-complementary investigations of thermophysical properties – high thermal resolution procedures in practice, *Proceedings of Thermophysics 2010*, pp.218-235, ISBN 978-80-214-4166-8, Valtice, 3nd÷5th November 2010

Perkowski, Z. (2011). A thermal diffusivity determination method using thermography: Theoretical background and verification. *International Journal of Heat and Mass Transfer*, Vol.54, No.9-10, (April 2011), pp. 2126-2135, ISSN 0017-9310

Phylippov, L.P. (1984). Temperature Wave Techniques, In: *Compendium of Thermophysical Property Measurement Methods. Volume 1: Survey of Measurement Techniques.* Plenum Press, K. D. Maglić, A. Cezairliyan & V. E. Peletsky (Eds.), ISBN 0-306-41424-4, New York, USA

Platunov, E.S. (1992). Instruments for Measuring Thermal Conductivity, Thermal Difusivity, and Specific Heat Under Monotonic Heating, In: *Compendium of Thermophysical Property Measurement Methods, Volume 2: Recommended measurement Techniques and Practices.* Plenum Press, K. D. Maglić, A. Cezairliyan & V. E. Peletsky (Eds.), pp. 337-365, Plenum Press, ISBN 0-306-41424-4, New York, USA

Ražnievič, K. (1966). *Thermal tables and charts*, (In Polish). WNT, Warsaw, Poland, (English edition: K. Raznjevic (1976). *Handbook of Thermodynamic Tables and Charts*, McGraw-Hill, Washington, ISBN 978-0070512702, Washington-New York, USA)

Rémy, B.; Degiovanni, A. & Maillet, D. (2005). Measurement of the In-plane Thermal Diffusivity of Materials by Infrared Thermography. *International Journal of Thermophysics*, Vol.26, No.2, (March 2005), pp. 493 – 505, ISSN 0198-925X

Sakagami, T. & Kubo, S. (2002). Applications of pulse heating thermography and lock-in thermography to quantitative nondestructive evaluations. *Infrared Physics and Technology*, Vol,.43, No.3-5, (June 2002), pp. 211-218, ISSN 0017-9310

Tye, R. P. & Salmon, D. R. (2005). Thermal Conductivity Certified Reference Materials: Pyrex 7740 and Polymethylmethacrylate. In: *Thermal Conductivity 26 / Thermal Expansion 14,* R. B. Dinwiddie, R. Mannello, (Eds.), 291-298, DEStech Publications, Inc., ISBN 1-932078-36-3, Lancaster PA, USA, pp. 437-451

Volokhov, G.M & Kasperovich, A.S. (1984). Monotonic Heating Regime Methods for the Measurement of Thermal Diffusivity, In: *Compendium of Thermophysical Property Measurement Methods,* K. D. Maglić, A. Cezairliyan & V. E. Peletsky (Eds.), pp. 337-365, Plenum Press, ISBN 0-306-41424-4, New York, USA

Wang, Z.I. & Tung, D.W. (2011). Experimental Reconstruction of Thermal Parameters in CNT Array Multilayer Structure. *International Journal of Thermophysics*, Vol.32, No.5, (May 2011), pp. 1013-1024, ISSN 0198-925X

Zhang, S.; Vinson, M.; Beshenich, P. & Montesano, M. (2006). Evaluation and finite element modelling for new type of thermal material annealed pyrolytic graphite

(APG). *Thermochimica Acta*, Vol.442, No.1-2, (March 15, 2006), pp. 6-9, ISSN: 0040-6031

Żmuda, S.; Panas, A. J.; Sypek, J. & Preiskorn, M. (2005). Validation of thermal diffusivity measurements of hard tissue specimens by finite element analysis, In: *Thermal Conductivity 27/ Thermal Expansion 15,* H. Wang , W. Porter (Eds.), pp. 113-120, DEStech Publications, Inc., ISBN 1-932078-34-7, Lancaster PA, USA

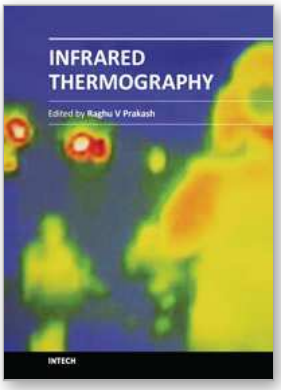

Infrared Thermography

Edited by Dr. Raghu V Prakash

ISBN 978-953-51-0242-7
Hard cover, 236 pages
Publisher InTech
Published online 14, March, 2012
Published in print edition March, 2012

Infrared Thermography (IRT) is commonly as a NDE tool to identify damages and provide remedial action. The fields of application are vast, such as, materials science, life sciences and applied engineering. This book offers a collection of ten chapters with three major sections - relating to application of infrared thermography to study problems in materials science, agriculture, veterinary and sports fields as well as in engineering applications. Both mathematical modeling and experimental aspects of IRT are evenly discussed in this book. It is our sincere hope that the book meets the requirements of researchers in the domain and inspires more researchers to study IRT.

How to reference

In order to correctly reference this scholarly work, feel free to copy and paste the following:

Andrzej J. Panas (2012). IR Support of Thermophysical Property Investigation - Study of Medical and Advanced Technology Materials, Infrared Thermography, Dr. Raghu V Prakash (Ed.), ISBN: 978-953-51-0242-7, InTech, Available from: http://www.intechopen.com/books/infrared-thermography/ir-support-of-thermophysical-property-investigation-medical-and-advanced-technology-materials-study-

INTECH
open science | open minds

InTech Europe
University Campus STeP Ri
Slavka Krautzeka 83/A
51000 Rijeka, Croatia
Phone: +385 (51) 770 447
Fax: +385 (51) 686 166
www.intechopen.com

InTech China
Unit 405, Office Block, Hotel Equatorial Shanghai
No.65, Yan An Road (West), Shanghai, 200040, China
中国上海市延安西路65号上海国际贵都大饭店办公楼405单元
Phone: +86-21-62489820
Fax: +86-21-62489821